Fire performance of blind-bolted connections to concrete filled tubular columns in tension

Ana M. Pascual [a], Manuel L. Romero [a]* and Walid Tizani [b]

[a] *Instituto de Ciencia y Tecnología del Hormigón (ICITECH),
Universitat Politècnica de València, Valencia, Spain*
[b] *Department of Civil Engineering, The University of Nottingham,UK*
* Corresponding author. e-mail address: mromero@mes.upv.es

ABSTRACT

This paper describes an advanced numerical model to predict the fire behaviour of blind-bolts in the tension area of endplate connections between I-beams and concrete filled tubular (CFT) columns. It is the continuation of a previous research on the thermal response of connections, considering the tension load of a moment-resisting connection. Due to the absence of experiments and data on blind-bolts fire performance the aim was to provide a model for their study. The effect of two main variables was researched, the concrete infill of the columns and the anchored extension of the blind-bolt. The fire resistance rating (FRR), the failure mode and the force-displacement-temperature curve at high temperatures were discussed. Results proved that concrete inside the column enhances the connections response at elevated temperatures in terms of FRR and stiffness. On the other hand, the use of anchored blind-bolts compared with normal blind-bolts provided stiffer connections, but the FRR improvement depended on the plate thickness and steel bolt properties. Finally, the use of fire resistant steel bolts as a method to enhance the fire response was assessed, observing the benefits to these connections when the shank of the blind-bolt governs the failure.

NOTATION

CFT	Concrete filled tube
EXP	Experimental
EHB	Extended Hollo-bolt fastener system
EC3	Eurocode 3. Part 1.2
EC4	Eurocode 4. Part 1.2
FEA	Finite element analysis
FEM	Finite element method
FR	Fire resistant
FRR	Fire resistance rating
f_c	Compressive cube strength of concrete at room temperature
f_y	Yield strength of steel at room temperature
f_u	Ultimate strength of steel at room temperature
NUM	Numerical simulation
HSS	Hollow steel section
HB	Hollo-bolt fastener system
UHB	Hollo-bolt in an unfilled section
ξ	Ratio of experimental to FEM results
μ	Friction coefficient

1. INTRODUCTION

In recent years, advantages of hollow section columns filled with concrete have been widely demonstrated. Hollow steel section (HSS) tubes are characterized by a higher torsional rigidity and better buckling strength compared with open section columns. Concrete infill enhances the structural behaviour, increases the strength of the column and prevents local buckling of the steel tube. On the other hand, steel provides a confinement to the concrete and improves its strength and stiffness. Moreover, additional benefits are obtained under fire conditions, due to the insulation and heat sink effect of concrete. However, the connection is a drawback hindering the use of CFT and the lack of suitable simple methods for its structural analysis helps to explain it. In that respect it is noted that the component method comprised in Eurocode 3 Part 1.8 [1] permits to obtain analytically the main structural characteristics of joints by assembling springs of the contributive parts. But, its use is still restricted to connections between steel open sections. Nevertheless, a significant effort is being made for the applicability in connections involving HSS and CFT columns [2-4]

The difficulty of the connection lies on the absence of access inside the tube that does not allow bolted connections with standard bolts. Primarily, the solution adopted by designers was welding, but execution and maintenance problems caused the development of blind-bolts, able to be tightened from one side of the tube. Up to now, several different blind-bolt systems have been designed, such as Flowdrill (Flowdrill B.V., The Netherlands), the Hollo-bolt (Lindapter International, UK) and the Ajax Oneside (Ajax Engineered Fasteners, Australia). As a rule, these systems provide simple connections, nonetheless, their capacity to resist moments transmitted by beams has been the aim of many researches [5-8].

Among these fastener systems, the present investigation deals with the Hollo-bolt system by Lindapter [9] and the Extended Hollo-bolt (Fig 1), which was a modified version of

the Hollo-bolt developed in the University o_f Nottingham [2, 10] that allowed the connections to bear bending moments. Three parts compound mainly the Hollo-bolt: a standard bolt, a sleeve with four slots and a cone with a threaded hole where the bolt is screwed, Fig 1a. It requires an easy installation: firstly, the piece is inserted through clearance holes of the elements to join, then, the bolt is tightened causing the cone to move against the inner face of the tube and the sleeve's legs expand until the total clamping force is transmitted.

The Extended Hollo-bolt (EHB) is a Hollo-bolt (HB) with a longer shank ended in a screwed nut, Fig 1b. Its purpose is to reduce the stress concentration in steel tube and distributing it within concrete in order to improve the stiffness connection. Tizani et al [11] carried out eight full scale tests on endplate connections between I-beams and CFT columns with Extended Hollo-bolts, through them the fastener system capability to provide semi-rigid connections was demonstrated. Recently, Pitrakkos and Tizani [2] accomplished an extended experimental program focused on Extended Hollo-bolt tensile behaviour within the framework of the component method.

The characterization of blind-bolted connections to tubular columns at ambient temperature has been the objective of several investigations, however, no researches have been found related to their fire performance. This is linked to the fact that traditionally, during a fire event, connections have been assumed to be colder than the elements jointed, due to its lower section factor A/V (exposed area A of the element per unit of length divided by V volume of the element per unit of length). Thus, the same protection as the rest of elements was normally used, nonetheless in several catastrophic fires [12, 13] the failure of the connection has been pointed out as the cause of the structural collapse. The limited understanding of connection fire performance and the oversight of the forces induced by the beams during the fire were the reasons for the building collapses.

4

First studies on the connection fire performance were on steel connections. For instance, the scarcity of data led Al-Jabri et al. [14] to conduct an experimental program on the fire performance of semi-rigid connections between steel open sections, which was completed with their FEM numerical simulation [15]. Further studies focused on the tying capacity and ductility of connections as the clue for the structure robustness at elevated temperatures. Yu et al.[16] and Huang et al.[17] undertook these aspects through an experimental program on flush steel endplate connections and steel beam to partially-encased H-section columns. Besides, Jiao-Ting et al. [18] investigated the axial force effect on flush endplate connection's capability in fire. Robustness was also the framework for the experimental and numerical analysis developed by Wang et al.[19] and Dai et al. [20], who assessed the behaviour at high temperatures of five different types of steel joints beam to columns. Fire exposure was maintained until the end of the test, when the tensile forces transmitted by restrained beam in catenary action caused the fracture of the connection. Concerning the fire behaviour of beam to CFT connections in realistic structures, five types of joints were studied by Ding and Wang [21] and Elsawaf et al. [22]. They demonstrated the importance of the connection flexibility and strength if the full capacity of the beam wanted to be achieved. Reverse channel connections were there highlighted due to their desirable ductility and were also the aim of Lopes et al. [3] research.

Some of the aforementioned studies on the fire performance of bolted connections assumed concrete filled tubular columns but none of them was taking into consideration blind-bolted connections and their fire behaviour. Hence, the purpose of this research is to obtain insight into the response at high temperature of blind-bolted moment-resisting connections, with the focus on the tension zone. A previous research from the authors [23]

deals with the thermal analysis of the connection, and this paper is the subsequent work that addressed the tension-deformational state produced by the tensile loading in fire.

This research is based on advanced numerical calculations using Finite Element Analysis (FEA). The finite element model of the connections mechanical performance at room temperature is validated with experiments from the literature [2, 10] and the thermal model with the work from the authors [23].

Simulations of connections to HSS and CFT are included, with Hollo-bolts and with Extended Hollo-bolts. In addition to the development of the models able to reproduce the connection fire response, the aim is therefore finding out the role of the concrete infill and the bolt anchorage within the concrete by comparison between the different types of connections. Finally, the effect of fire resistant (FR) steel bolts is considered as a method of increasing the fire exposure time, or Fire Resistance Rating (FRR), before the connection collapse.

2. VALIDATION OF THE NUMERICAL MODEL

2.1. Introduction

This section reports on the validation method of the numerical calculations of the two connections under study, which are shown in the Fig 2 and Fig 3. Three-dimensional numerical models were developed using the FEA package ABAQUS [24]. The thermo-mechanical response of the connections was based on separate thermal and the mechanical calibrated models that are presented in the following subsections.

Pascual A M, Romero M L, Tizani W. Fire performance of blind-bolted connections to concrete filled tubular columns in tension. Engineering structures 2015;96:111-125. http://dx.doi.org/10.1016/j.engstruct.2015.03.06

2.2. Blind-bolted connections at room temperatures.

2.2.1. Benchmark studies

Multiple processes take place during connection loading as a consequence of the interaction of several components that possess different non-linear material properties. The stick and slip of the surfaces, the pull-out and the post-yield behaviour are complex phenomena to be captured and involve many convergence problems. Therefore, in addition to the mechanical model of the two configurations (Fig 2 and Fig 3) representatives of the tension area of a connection between I-beam and CFT, other connections were modelled (Table 1). The objective was to ensure with a large number of simulations the adequacy of the final models used for the thermo-mechanical analysis. Table 1 lists the connections used for the calibration at room temperature [11, 25-28]. Simpler models with standard bolts and only steel elements were first developed, as good correlation was being obtained, the calibration process moved to more complex connections, with the blind-bolt fastener system, the hollow section column and finally, the concrete core filling the tube column. Two of these preliminary cases are presented in Fig 4, which depicts the FEM model and the comparison between the FEM moment-rotation curve and the experimental curve. Fig 4a and 4b shows an endplate connection between an I-beam and a HSS column [28], and Fig 4c and 4d an endplate connection between an I-beam and a CFT column [11]. The simulations provided good accuracy with test results. A proof of it is the ratio of experimental to FEM results at maximum load, ξ, which pointed out differences lower than 10%, Table 1.

The adequate correlation with the experiments led to undertaking the modelling of the two connections shown in Fig 2 and 3, whose definition was based on the experiments used for the validation [2, 10].

2.2.2. Description of the FE model

The first connection under study consisted of a single blind-bolt clamping a loading frame plate and the tube column, Fig 2. Tensile force was transmitted to blind-bolts through the rigid loading frame plate, 30 mm thick. The tube column was not strictly a real commercial HSS, it was an arrangement of plates that worked similarly and where the upper plate was 20 mm thick. The thickness of the plates was designed in order to behave in the elastic range and in consequence, all attention was focused on blind-bolts performance which controlled the behaviour of the connection. An overall of 8 specimens from Pitrakkos and Tizani [2] were simulated, Table 2.

The second connection to evaluate involved two T-stubs bolted to opposite sides of a HSS 200x200x10 S375 taken from Ellison and Tizani [10], Fig 3. As in the specimen with the single blind-bolt the main interest was concentrated on the blind-bolt behaviour, so thickness of T-stub flanges was 50 mm. Load was applied by pulling out the upper T-stub while the bottom one was maintained fixed. Two specimens were calculated and validated, considering the connection to a concrete-filled tubular (CFT) column with the two different fastener systems: the Hollo-bolt and the Extended Hollo-bolt, Table 2.

The definition of the finite element model for both connections followed essentially the same criteria, Fig 5a and Fig 6a depicts the model of each connection. They were symmetrical about the vertical planes, so only quarter of the specimens was simulated in order to reduce the computational cost.

The fastener system was modelled in the tightened state, i.e. assuming the sleeve shape and fastener cone position after the torque application, Fig 5a. Hollo-bolt was simplified into two parts: the first one included the standard M16 grade 8.8 and the fastener cone, the second one represented the sleeve in the expanded state. The shank length was 100 mm in the single

blind-bolted connections and 120 mm length in the double T-stub connections. The Extended Hollo-bolt was similarly modelled (Fig 5a), by means of the two parts, but taking into account the longer shank (150mm long for both connections) and a nut attached at the end. For the sake of simplicity, the screw thread in the bolt shank was not considered, nor the hexagonal shape of the bolt head and nut.

The analysis procedure attempted to reproduce the actual execution steps of the specimen. In the first stage and before the concrete fill took place, the torque was applied using the ABAQUS "bolt load" function. In the second step, the concrete was inside the tube and the tension load was transmitted through the loading frame plate or the upper T-stub as a static displacement. The failure took place when the velocity of the deformation increased abruptly, which coincided with the lack of equilibrium in the system and the loss of convergence of the Newton's method.

Three-dimensional eight-noded solid elements with reduced integration (C3D8R) were employed for all the parts in the connection. Mesh density was finer in areas where higher stress gradient occurred, i.e. around blind bolts, where most interactions happened. Conversely, mesh size increased in the zones where lower stress and strain concentration was expected.

Due to the multiple and different parts in contact, the complexity of the numerical model resided to a greater extent in the interactions definition. A total of 9 contacts were tackled which could be classified into two groups:

a) Contacts between steel surfaces: headbolt to plate/T-stub flange, sleeve to plate/T-stub flange hole surface, sleeve to tube column hole surface, sleeve to fastener cone and external face of tube column to plate/T-stub flange.

Pascual A M, Romero M L, Tizani W. Fire performance of blind-bolted connections to concrete filled tubular columns in tension. Engineering structures 2015;96:111-125. http://dx.doi.org/10.1016/j.engstruct.2015.03.06

b) Contacts between steel and concrete surfaces: internal face of the steel tube column to concrete, sleeve to concrete, shank to concrete and nut to concrete (when Extended Hollo-bolt is used).

Interactions were defined as surface to surface contact with finite sliding formulation. In normal direction, "hard" contact behaviour was used, whereas in the tangent direction the Coulomb friction model was employed.

By means of the friction coefficient (μ), coulomb friction law relates the maximum shear stress in the surfaces with the pressure between them, it was assumed 0.25 in the interaction steel-concrete [29]. In the case of steel-steel contacts the values observed in the bibliography for the friction coefficient went from 0.25 of Bursi and Jaspart [25] to 0.44 of Shi et al. [30] and 0.5 used by Cabrero [31]. Eventually, $\mu=0.25$ was used in steel-steel contacts except for sleeve to fastener cone interaction and sleeve to tube hole where was necessary to increase the sticking area increasing the friction coefficient, otherwise slippage of surfaces introduced bolt motion and made the convergence difficult. On the one hand, sleeve to fastener cone interaction used 0.5 friction coefficient for single blind-bolt connections and 0.35 in the double T-stub connections, and on the other hand, sleeve to tube hole friction coefficient was 0.8 and 0.5 respectively. Besides the convergence, these values were justified by a sensitivity analysis, comparing force-displacement curves with experimental curves. Figure 7 shows the effect of using $\mu=0.8$ or $\mu=0.5$ for the contact between sleeve and plate hole surfaces in the single blind-bolt connection, correlation accuracy was enhanced with $\mu=0.8$.

2.2.3. *Material models at room temperature*

Steel

The plasticity model for steel behaviour was isotropic multiaxial with the Von Mises yield surface. Linear behaviour was defined through Young's modulus (E) and Poisson ratio's (ν). Material starts yielding when yield strength, f_y, is reached

Standard bolts that formed the fastener system were high strength steel M16 (16 mm diameter) grade 8.8. The first digit is the value of ultimate strength (f_u= 800 MPa) and the second one indicates the portion of ultimate strength that represents the value of yield strength (f_y= 640 MPa). Nonetheless, strain-stress curve was defined by means of the data from tests used for the validation [2, 10].

Sleeve specifications are provided in the Lindapter catalogue [9]. Sleeve length depends on the total thickness to fasten, i.e. the plate plus the tube thickness. In the single blind-bolted connections (30+20= 50 mm) 63 mm sleeve length was prescribed and 84 mm in the case of the T-stub connections (10+50=60mm). Regarding sleeve strength, 430 MPa are indicated in the catalogue, although values of yield and ultimate strength from experimental data available in the literature [32] were finally adopted. In a similar way, structural steel for tube section was of grade S355 but again values of strength were extracted from data test on analogous tubes [11].

Table 3 indicates the engineering values of strength used and the source of them. Nevertheless, instead of using the engineering stress-strain curve, the true stress-strain curve was applied, considering the change in material volume beyond the yield limit.

$$\sigma_t = \sigma_e(1+\varepsilon_e) \tag{1}$$

$$\varepsilon_t = \ln\ (1+\varepsilon_e) \tag{2}$$

Concrete

The concrete damaged plasticity model was selected to define the yielding part of the concrete. Elastic behaviour of concrete was isotropic and linear, but once the material reached

the yield surface it followed a non-associated plastic flow and the flow potential is the Drucker Prager hyperbolic function. The parameter values that described the yield surface and plastic flow were obtained from literature [33]. For the dilation angle (ψ), which defined the dilatancy in plasticity, 30º and 15º were used. Due to the confinement effect was not important in the specimens of this research, there were no difference between the two dilatancies. The default value for the ratio (K), which informed about shape of the deviatory plane was 0.66. A value of 0.8 was also studied, obtaining similar results. The other three parameters that complete the model definition were: eccentricity ($\epsilon=0.1$), ratio of initial equibiaxial compressive stress to initial uniaxial yield stress ($f_{b0}/f_{c0}=1.16$) and viscosity parameter (0.01).

The damaged plasticity model permitted the definition of the plastic regimen under compression and tension. For concrete compression, the stress-strain hardening and softening curve was obtained from Eurocode 2 Part 1.1 [34]. The post failure tension behaviour was defined by stress-fracture energy law [35]. Concrete of grade C40 was used in specimens with a single blind-bolt, and C50 in the double T-stub connections.

2.2.4. *Results and validation*

Single blind-bolted connections

Eight connections consisted of a single bolt were modelled (Table 2. Specimens notation from [2] was maintained). The bolt displacement and the force applied to the system, calculated by means of the reaction forces, were controlled through simulation. Fig 5b shows the force-displacement curves for two of the specimens and their correlation with test data. The change of stiffness depending whether the blind-bolt was the Hollo-bolt or the Extended Hollo-bolt was detected (Fig 5b), besides Mises stress revealed the crushing of the concrete

and stresses concentration in the sleeve in the HB connections. Thus, the stiffness enhancement due to the EHB was correctly captured by the FEM model. It was also observed that all connections finally failed by the fastener system, more specifically due to the bolt shank fracture. Table 2 indicates the maximum load values reached by the numerical model ($N_{u, FEM}$) and tests ($N_{u, test}$). The ratio ξ indicated differences not greater than 5% in HB and EHB, 8% for HB in the unfilled column connection and 11% for the standard bolt M16.

Double T-stub blind-bolted connections to tube columns

The double T-stub connections to CFT involved a total of 8 blind-bolts. Their performance at room temperature was calibrated for two specimens (Table 2). The pull out load was applied to the upper T-stub by means of imposed displacements. At the same time, the displacement under evaluation was the separation of the two T-stub flanges. Figure 6b shows the good correlation of curves force- plate separation with the test data. Despite the thickness of the tube was thinner than in the one bolt connection, the failure was still controlled by the bolt shank capacity. The Extended Hollo-bolt system again exhibited higher stiffness than the Hollo-bolt, due to the anchorage. The anchored nut, through stress distribution within the concrete, reduced the crushing around the sleeve detected in HB. The ratio ξ for the maximum load reflected differences not higher than 3%, as it can be observed in Table 2.

2.3. Thermal behaviour of the blind-bolted connections

The thermal behaviour of blind-bolted connections was studied by the authors in a previous work [23], through experiments and FEA. The laboratory program consisted of twelve unloaded small-scale specimens, which were exposed to the standard fire curve ISO834 [36] in a gas furnace, Fig 8a. Three types of connections were analyzed: using Hollo-

bolt system to connect a plate with an unfilled tube column (HSS), the same blind-bolt but in a filled tube (CFT) connection and the Extended Hollo-bolt in a CFT. Measurements of temperature were taken at different positions of the bolt and across the concrete section. In parallel, three-dimensional numerical model for the connections were developed to simulate the pure heat transfer problem. Thermal properties of the material and interactions were calibrated through comparison with the experiments.

As a result, accurate simulations of the thermal behaviour were accomplished. Fig 8b shows the correlation for the case of EHB fastener system between temperature-time curves calculated numerical and experimentally.

3. FIRE PERFORMANCE UNDER TENSION

3.1. Introduction

Once mechanical and thermal numerical models proved to be able to capture the connections behaviour with reliability, the fire analysis was carried out. The two blind-bolted connections representatives of the tension area in moment-resisting connections were studied under tensile load and elevated temperatures: the single blind-bolted connection and the double T-stub connection to the tube column, Fig 2 and 3. Three cases were conducted for each one: with HB and HSS column, HB and CFT column, and EHB and CFT column, Table 4.

3.2. Description of the FE model

3.2.1. Analysis Procedure

The geometry of the connections defined for the analysis at room temperature was maintained (section 2.2.2).

Pascual A M, Romero M L, Tizani W. Fire performance of blind-bolted connections to concrete filled tubular columns in tension. Engineering structures 2015;96:111-125. http://dx.doi.org/10.1016/j.engstruct.2015.03.06

Sequentially coupled thermal-stress analysis were carried out, following the recommendations of Espinos et al [37]. In this type of analysis the stress-strain solution depended on the temperature field but not the opposite. Conversely, in a fully coupled analysis, the mechanical and thermal response affect each other, the stress and thermal analysis are simultaneous. The latter procedure is closer to reality, but at the expense of high computational cost and convergence problems, the accuracy improvement is not worth nothing hence.

In a sequentially coupled thermal-stress analysis two finite element models are needed: a thermal model and a mechanical model. First, the pure heat transfer model was computed. Temperature-time curves were obtained for each node and kept to be applied to the mechanical model as a prescribed thermal load after the axial loading. Afterwards the mechanical model for the stress-deformation was developed. Before tensile load application, the stress produced in the steelworks by tightening the bolts was input as an initial state. In the following stage, and taking into account that the tube is filled with concrete, load was applied. Finally, the temperature field kept was input onto the mechanical model while the load was propagated.

Thermal analysis

The nonlinear heat transfer analysis was first conducted for each connection. External surfaces of connections were exposed to the standard ISO834 fire curve [36], that acted as a thermal load by means of convection and radiation heat transfer mechanisms. Through the connection elements, conduction was the main heat transfer mechanism. Three-dimensional eight-noded heat transfer brick elements were used with nodal temperature degree of freedom DC3D8.

Pascual A M, Romero M L, Tizani W. Fire performance of blind-bolted connections to concrete filled tubular columns in tension. Engineering structures 2015;96:111-125. http://dx.doi.org/10.1016/j.engstruct.2015.03.06

Thermal properties for concrete, i.e. specific heat and thermal conductivity, were taken from EC4 Part 1.2 (EC4) [38]. A moisture content of 3% in concrete weight was assumed to define the peak value in the specific heat, which represents the latent heat of water vaporisation recommended by EC4 [38] in the absence of experimental data.

High strength steel bolts behave differently dependent on the chemical composition and heat treatment in the fabrication. In a preceding paper by the authors [23], the limited data relating to thermal properties of high strength steel bolts at elevated temperatures was noted. The authors verified the small differences between the thermal properties from steel bolts tested by Kodur [39] and the ones from EC3 Part 1.2 (EC3) [40]. For this reason, the temperature dependent thermal properties from EC3 [40], based on mild steel tests, were finally used to define all steel.

Regarding thermal interaction characteristics between the different parts of the connections, perfect contact was assumed, except for the sleeve to the plate hole surface and the internal surface of steel column to the concrete infill. In these contacts a thermal conductance gap of 200 W/m^{2}K was adopted, following the recommendations drawn from [23].

Structural analysis

A nonlinear stress analysis was subsequently conducted, where tensile load was applied to the blind-bolts. Before loading, bolt pretension was introduced by means of an initial stress-strain state in the steelwork as a result of the bolt tightening. Later on, the connections were subjected to the tension load (50% maximum load at room temperature) and, at the ultimate stage, nodal temperature-time curves from the thermal model were input. The finite element meshes and the node numbering were exactly the same for the different models used

Pascual A M, Romero M L, Tizani W. Fire performance of blind-bolted connections to concrete filled tubular columns in tension. Engineering structures 2015;96:111-125. http://dx.doi.org/10.1016/j.engstruct.2015.03.06

for the thermo-mechanical analysis. Three-dimensional eight-noded elements were employed with three degrees of freedom (C3D8R).

A surface to surface contact was defined for the interactions between the different parts of the connection. In the normal direction, a 'hard' contact model was used whereas in the tangent direction Coulomb friction model was defined, similarly to models at room temperature.

3.2.2. *Mechanical material properties at elevated temperatures*

Mechanical properties of steel and concrete vary with temperature. In the case of the steel, normal steel and high strength steel bolt have different response at elevated temperatures. EC3 [40] provides the stress-strain relationship and the reduction coefficients (Fig 9) for normal steel, dependent on the temperature, to affect the values at room temperature (yield strength f_y, proportional limit f_p and Young modulus E). In addition, in its Annex D recommends specific strength reduction factors for steel bolts, which are based on research done by Kirby [41].

Figure 10 shows the true stress-strain curve for the steel bolts in the single blind-bolted connection at different temperatures, so, as in room temperature the reduction of the volume was considered. Reduction factors from EC3 Annex D [40] and strain hardening from EC3 Annex A [40] were also applied. Concerning the expansion coefficient for steel, it was extracted from EC3 [40] as well

For the concrete, the stress-strain relationship and the expansion coefficient at elevated temperatures were defined following Eurocode 2 Part 1.2 [42].

3.3. Results

The data obtained through the numerical calculations of both types of connections was analysed, taking into account the stress-strain distribution and the temperature field. The main findings were related to the mode of failure and the FRR, which provided an estimation of the controlling element of the connection failure and the fire capacity.

The comparison of the results between the three types of connections, i.e., the HB to the HSS, the HB to the CFT and the EHB to the CFT, aided the assessment of the concrete effect and the influence of the anchorage.

3.3.1. Fire behaviour of single blind-bolted connections

Failure mode

As it is mentioned in section 2.2.2 of this paper, the plate and tube thickness were designed in order that the connections failed as a consequence of the fastener system fracture. Nevertheless, two parts of the fastener system were able to determine the response: the shank of the bolt and the sleeve. Depending on the type of connection, the failure was governed by one of them. In case of being dominated by the sleeve, strength was lower but flexibility higher.

Figures 11a and 11b compare Mises stresses along the shank bolt and the sleeve with their respective steel strength capacity (f_u), immediately before the collapse and for the three types of connections. They show the part of the connection (shank or sleeve) that reached the ultimate capacity and indicate the section where failure was assumed and which coincides for all of the connections. For the shank bolt, the critical section was next to the bolt head (Fig 11a), where temperature was highest and, consequently, steel strength is lowest. Meanwhile, in the sleeve, the highest stresses were concentrated around the folded section, Fig 11b.

18

Figures 11a and 11b include a second axis that reflects the temperature along both parts. It can be observed that fracture occurred around 500ºC, when steel strength decrease became more significant and was reached by Mises stress.

In the HB connection to the HSS column, sleeve and shank failed at the same time, Fig 11a and 11b. However, in connections to CFT columns (HB and EHB) the failure was dominated by the shank fracture, due to the fact that stresses distributed through the concrete reducing sleeve deformation. Finally, the ultimate strength capacity of the shank bolt was reached in all of the three connection types.

Fire resistance rating

The Fire Resistance Rating (FRR) indicates the time in minutes that the connection is capable of sustaining the loads before failure. The single blind-bolted connections were calculated under different load levels with regard to the maximum load supported at room temperature, in order to know its influence on the FRR. Table 5 shows that FRR increased by 11 minutes for the three connections types when load level decreased from 50% to 20% load level. Expectedly, as the load level was lower, the FRR improved. Moreover, it is worth noting that unprotected connections to CFT columns reached 36 min of FRR when 20% loaded (Table 5).

The effect of concrete on bolt temperature can be observed from Fig 11a by inspecting the area of the bolt directly in contact with concrete, starting from 0.08 m along the shank length. However, the shank bolt fracture occurred next to the exposed area of the bolt, so concrete influence was not as remarkable as it was expected. Connections to CFT gained 4-5 min (16-20%) of FRR compared with HSS connections, Table 5. The heat sink effect of concrete was assumed to be more important in case of thinner tube and plate.

19

Pascual A M, Romero M L, Tizani W. Fire performance of blind-bolted connections to concrete filled tubular columns in tension. Engineering structures 2015;96:111-125. http://dx.doi.org/10.1016/j.engstruct.2015.03.06

On the other hand, there were no differences in FRR between the Hollo-bolt and the Extended Hollo-bolt connection to CFT, Table 5. Similarly, it was attributed to the fact that the fracture took place next to the head of the bolt and the bolt anchorage within the concrete did not reduce stress nor temperature in that section.

3.3.2. *Fire behaviour of double T-stub connections to tube columns*

Failure mode

The FEM model of the double T-stub bolted connections permitted to gather more data to understand the connection fire performance. Thickness of the T-stub flange was designed to eliminate any influence on the behaviour, however, the tube thickness was significantly lower than in the single blind-bolted connections, so its effect should not be totally neglected.

Figure 12 shows the deformed shape at failure of the double T-stub connections at elevated temperatures. Concrete prevented the deformation of the tube column that took place in the HSS, as it occurred at room temperature. Plastic deformation is also depicted in Fig 12, which helped for the detection of the failure mode for each type of connection. In the connection to the unfilled column, stress on the sleeve governed the failure whereas the shank did not present plastic deformations (Fig 12a). In the case of CFT columns, bolt shank reached its ultimate capacity and dominated the connections collapse, although high plastic strains were also observed in the sleeve and the concrete (Fig 12b and 12c).

Compared to the connection with the single blind-bolt, stress distribution through concrete was limited by the tube column and deformation of tube introduced a new factor to be further considered.

Fire resistance rating

Pascual A M, Romero M L, Tizani W. Fire performance of blind-bolted connections to concrete filled tubular columns in tension. Engineering structures 2015;96:111-125. http://dx.doi.org/10.1016/j.engstruct.2015.03.06

The FRR enhancement in connections filled with concrete can be observed in Table 5. FRR increased by around 4 min relative to unfilled columns, which meant 25% increase. On the other hand, no differences were detected between the Hollo-bolt and the Extended Hollo-bolt response. In the latter, the part of the bolt deepest embedded in concrete was colder, but it had no effects on the temperature of the bolt fracture section. Similarly to the single blind-bolted connection, the bolt collapse occurred next to the head of the bolt shank.

4. PARAMETRIC STUDY

4.1. Introduction

The versatility of the numerical model permitted determining the influence of different parameters on the connection performance. Firstly, the properties of steel bolts were varied considering the works from Kodur et al [39] on the steel capacity at the same time that the benefits of using Fire Resistant bolts were proved. In the second place, the procedure of analysis was changed into steady-state analysis to determine the connection response at certain temperatures.

4.2. Properties of steel bolts

Properties of the high strength steel bolt of the fastener system at elevated temperatures determine to a greater extent the fire response of the connection. Although EC3 Annex D [40] propose a strength reduction factor for high strength steel bolt, the necessity of further research has been noted by several authors. Kodur et al [39] carried out laboratory tests on Grade A325 (f_y= 630MPa, f_u=830MPa) and A490 bolts (f_y= 895MPa, f_u=1030MPa). They obtained data that permitted the development of analytical expressions to characterise the thermal and mechanical properties of high strength steel bolt at elevated temperatures. Figure

Pascual A M, Romero M L, Tizani W. Fire performance of blind-bolted connections to concrete filled tubular columns in tension. Engineering structures 2015;96:111-125. http://dx.doi.org/10.1016/j.engstruct.2015.03.06

13a depicts the reduction factors using Kodur's proposals [39], compared with EC3 [40], meanwhile, Fig 13b shows comparison between elongation definitions. The effect of using Kodur properties [39] on the fire response is assessed below. Moreover, Gonzalez and Lange [43] tested grade 10.9 bolts, their aim was proving that the chemical composition and heat treatment during the manufacture influenced the high temperature response. Experiments gave a lower strength ratio in comparison with strength reduction factor from EC3 Annex D [40]. Hanus et al. [44] performed test on grade 8.8 bolts under heating-cooling cycles, this data was used to adjust a stress-strain law for high strength steel bolt affected by the maximum temperature reached and the final temperature of the test. Li et al [45] carried out test on 20MNTiB steel (f_y= 940MPa, f_u=1040-1240MPa), based on the test data they highlighted the different performance depending on the type of steel bolt and developed the subsequent equations for the steel properties.

In the present work the influence on FRR of using Kodur's proposals [39] for bolts A325 was evaluated, modifying properties of the steel bolts for the single blind-bolted connections. Fig 13a shows that the reduction factor by Kodur [39] is over the recommendations of Annex D [40] up to 450ºC, but never again beyond this temperature. Concerning the temperature in the shank fracture section at the collapse, it was around 500º (Fig 11), so reduction factor from Kodur [39] is under the Annex D [40] value and subsequently the FRR was two minutes lower, Table 6. Therefore, from 450ºC, the proposal from Kodur [39] was more conservative, but it did not represent important differences.

4.2.1. Fire Resistant steel bolts

Regarding steel bolt properties, the use of fire resistant (FR) steel bolts was also assessed as a method to enhance the connection behaviour at elevated temperatures. Their

Pascual A M, Romero M L, Tizani W. Fire performance of blind-bolted connections to concrete filled tubular columns in tension. Engineering structures 2015;96:111-125. http://dx.doi.org/10.1016/j.engstruct.2015.03.06

chemical composition and heat treatment allow better strength retention than in normal high strength steel. FR steel was a demand of steel manufacturers in Japan two decades ago and hence Sakumoto et al. [46] developed an experimental program testing the tensile and shear strength of FR steel bolts for FR steel constructions. Figure 14 shows the reduction factors for the FR steel bolts from Sakumoto et al. [46] under tensile load and the ones for high strength steel bolts from EC3 Annex D [40]. It can be observed that at 500ºC the reduction factor from Annex D [40] is 0.55 while experiments by Sakumoto et al. [46] exhibit a value of aprox. 0.75, so tensile strength is significantly higher for FR steel bolts. The FRR improvement for the blind-bolts connections is presented below.

Effect of FR steel bolts on single blind-bolted connections

In single blind-bolted connections to CFT the FR steel bolts provided 4 min FRR increase compared with normal steel, that meant FRR 16% enhancement in the case of using HB fastener system and 20% for EHB, Table 6. When the tube column was HSS the FRR improvement was around 1 min because the failure was dominated by the sleeve. In conclusion, when the shank of the blind-bolt governed the connection collapse, the enhancement provided by the FR steel bolt was not high, but it should be taken in consideration as a further method to comply with certain structural fire resistance requirements.

Moreover, the use of FR steel bolts in addition to the concrete infill increased the differences in FRR between connections to HSS and CFT, Table 6. FR steel bolts in CFT connections represented 35% FRR improvement compared with connections to HSS.

Effect of FR steel bolts on T-stub connections to tube columns

The FRR enhancement provided using FR steel bolts was also evaluated for the double T-stub connections. For connections to unfilled columns, the use of FR steel bolts did not

23

Pascual A M, Romero M L, Tizani W. Fire performance of blind-bolted connections to concrete filled tubular columns in tension. Engineering structures 2015;96:111-125. http://dx.doi.org/10.1016/j.engstruct.2015.03.06

result in any improvement. The sleeve was the most damaged element and determined the FRR, therefore, the use of FR steel bolts did not have any influence (Table 6). In connections to CFT column and Hollo-bolts as the fastener system, FRR increased by 2 min. The enhancement of the bolt steel strength made the fracture move from bolt shank to sleeve, which was capable to resist the load only 2 minutes more than in the case of normal high strength steel bolts. Conversely, in the connection to CFT with EHB, the FRR increased by 36% compared with normal high strength steel bolts. The anchorage distributed stresses through the concrete, so that, stress did not concentrate in the sleeve, and the bolt shank dominated the connection failure.

To conclude, in the case that tube thickness was not rigid enough to neglect its contribution to the connection fire performance, the effect of the anchorage and the use of FR steel bolts can be significant and requires a further study. Moreover, the combination of concrete filling the column, EHB as a fastener system and FR steel bolts represented 69.48% improvement compared with HB to a HSS, i.e. FRR increased from 17.78 min to 30.13 min.

4.3. Steady-state analysis of blind-bolted connections at 450ºC and 550ºC

At room temperature, concrete in CFT columns and anchorage by EHB increase the tensile stiffness of the connection [2, 10]. At high temperature, materials deteriorate introducing new connection behaviour patterns. In order to assess the strength and stiffness reduction of the connection as a consequence of materials weakening, the force-displacement curves for the two connections at a certain temperature (450ºC and 550ºC at the head of the bolt) were obtained. For this analysis, steady-state calculations were carried out. Instead of loading the connection up to a constant load and exposing it to a uniform temperature increase, connections were first heated linearly (2ºC/min) to the specified temperature, and

then, at constant temperature, load was applied until failure. Both, the single blind-bolted connections and the double T-stub connections, were analysed at 450ºC and 550ºC and compared with the behaviour at room temperature (20ºC). High strength steel bolts were employed using reduction factors from EC3 Annex D [40].

4.3.1. Force-displacement-temperature curve for single blind-bolted connections

Figure 15 shows the force-bolt displacement curve for the single blind-bolted connections, considering HSS and CFT columns, HB and EHB fastener system. Differences in stiffness between the three connection types that appeared at room temperature were also observed at 450ºC and 550ºC. The highest stiffness was therefore presented by connections with EHB, due to the anchorage, and secondly by HB in connections to CFT column. Concrete still increased its influence at high temperatures, even more due to its better behaviour at elevated temperatures in comparison with steel. This conclusion was not so evident for the HB connection to the CFT, because an initial slip attributed to model definitions modified the trend, but the overall curve confirmed the findings. Moreover, Fig 15 shows that stiffness of the EHB to CFT connection at 550ºC is similar to the stiffness of the HB to HSS connection at room temperatures, so the improvement due to the concrete was substantial. Concerning the maximum strength, it was governed by the steel bolt strength except for the connection to the unfilled section at 450ºC and 550ºC where the failure occurred before bolt shank fracture.

4.3.2. Force-displacement-temperature curve for T-stub blind-bolted connections

Similar conclusions were obtained for the double T-stub connections, as can be observed in Fig 16, where load-plate separation curves were depicted. At room and high temperature, stiffer connections were attained when hollow section was filled with concrete

Pascual A M, Romero M L, Tizani W. Fire performance of blind-bolted connections to concrete filled tubular columns in tension. Engineering structures 2015;96:111-125. http://dx.doi.org/10.1016/j.engstruct.2015.03.06

and using Extended Hollo-bolt instead of Hollo-bolt. Connection strength was governed by bolt shank strength, except for connection to the unfilled section at room temperature. However, at 450ºC and 550ºC, the ultimate capacity of the shank was reached in all them. Stiffness in connections to CFT (HB and EHB) at 550ºC was higher than stiffness in connections to HSS at room temperature, Fig 16.

This analysis reveals that stiffness enhancement due to concrete infill and anchorage is also observed at high temperatures, the increase was assumed even higher than at room temperatures, nonetheless it requires a further study. On the other hand, stiffness achieved in connections with EHB at 550ºC is similar to stiffness in connections to HSS at room temperature, which highlighted the benefits of the concrete and the bolt anchorage.

5. SUMMARY AND CONCLUSIONS

The present research is a numerical study on the fire performance of blind-bolted connections to CFT and HSS in the tension zone of moment-resisting connections. In the absence of fire experiments to validate the thermo-mechanical model, the mechanical part of the problem was corroborated at room temperature with tests on the same connections, whereas the validation of the heat transfer was accomplished in a preceding research by the authors [23].

The objective was to provide data to gain insight into tensile loaded blind-bolted connections in fire and to assess the effect of concrete infill and the anchorage of the blind-bolt. Two types of connections were analyzed, a single blind-bolt connecting a plate to a tube column and a double T-stub connection to a tube column. The type of column (HSS and CFT) and the type of fastener system (HB and EHB) were the variables considered for each connection. The fastener system was the element that governed the connection failure due to

the thickness of the plate or T-stub flange and the tube, but depending on the connection and temperatures, the sleeve or the bolt shank were determinant. The conclusions from the study are the following:

- Concrete filling the tube column resulted in 16-20% enhancement in FRR for the connection with the single bolt compared with connections to unfilled columns, and around 25% for the double T-stub connections. In connections to HSS, the failure was shared by the sleeve and the shank of the fastener system. For the connections to CFT columns the shank bolt of the fastener system decided the connections collapse, where stresses in the sleeve were lower due to the concrete.

- The anchorage of the shank bolt into the concrete provided by the EHB did not represent an increase in the FRR compared with the HB in connections to CFT. Failure of the shank was localised next to the bolt head where neither temperature nor stress were directly affected by the anchorage.

- The use of FR steel bolts was assessed as a method to improve the FRR. For the connections to HSS, FR steel bolts did not involve any benefit because the failure was dominated simultaneously by the sleeve, and its properties did not change. In the single blind-bolted connections to CFT, 15-20% improvement related to normal high strength steel was obtained for HB and EHB, respectively. In the T-stub connections when HB was the fastener system, the failure changed from shank to sleeve and a slight FRR increase of 2 min was achieved. Nevertheless, in T-stub connections with EHB, the anchorage reduced stress concentration in the sleeve and FR steel bolts governed the failure and meant 36% (8min) improvement in FRR compared with the use of normal high strength steel bolts. So, the effect of the FR steel and the anchored blind-bolt was more significant when column tube was thinner.

- The force-displacement curves for the CFT connections using EHB at 450ºC and 550ºC demonstrated that stiffness enhancement observed at room temperature, extended to high temperatures. The anchorage of EHB permitted stiffer connections due to better stress distribution. Besides, concrete reduced tube deformation and sleeve damage, consequently, it also enhanced stiffness. It is worth noting that connections to CFT were capable of achieving the same stiffness at 550ºC as connections to HSS at room temperature.

Further work in the laboratory will be carried out to corroborate the results and include a wider range of parameters.

REFERENCES

[1]   CEN. *EN 1993-1-8, Eurocode 3: Design of steel structures. Part 1-8: Design of joints.* Brussels, Belgium: Comité Européen de Normalisation. 2004.

[2]   Pitrakkos T, Tizani W. Experimental behaviour of a novel anchored blind-bolt in tension. Engineering Structures 2013. 49(0): 905-919.

Pascual A M, Romero M L, Tizani W. Fire performance of blind-bolted connections to concrete filled tubular columns in tension. Engineering structures 2015;96:111-125. http://dx.doi.org/10.1016/j.engstruct.2015.03.06

[3]   Lopes F, Santiago A, Da Silva LS, Heistermann T, Veljkovic M, Da Silva JG. Experimental behaviour of the reverse channel joint component at elevated and ambient temperatures. International Journal of Steel Structures 2013. 13(3): 459-472.

[4]   Da Silva LS, Neves LFC, Gomes FCT. Rotational stiffness of rectangular hollow sections composite joints. Journal of Structural Engineering-Asce 2003. 129(4): 487-494.

[5]   France JE, Davison JB, Kirby PA. Strength and rotational stiffness of simple connections to tubular columns using flowdrill connectors. Journal of Constructional Steel Research 1999. 50(1): 15-34.

[6]   France JE, Davison JB, Kirby PA. Strength and rotational response of moment connections to tubular columns using flowdrill connectors. Journal of Constructional Steel Research 1999. 50(1): 1-14.

[7]   France JE, Davison JB, Kirby PA. Moment-capacity and rotational stiffness of endplate connections to concrete-filled tubular columns with flowdrilled connectors. Journal of Constructional Steel Research 1999. 50(1): 35-48.

[8]   Lee J, Goldsworthy HM, Gad EF. Blind bolted T-stub connections to unfilled hollow section columns in low rise structures. Journal of Constructional Steel Research 2010. 66(8-9): 981-992.

[9]   Lindapter. Type HB - Hollo-Bolt. Cavity fixings 2, Product brochure. Lindapter International, UK. 2012: p 41-3.

[10]   Ellison S, Tizani W. Behaviour of blind bolted connections to concrete filled hollow sections. The Structural Engineer 2004. 82: 16-17.

Pascual A M, Romero M L, Tizani W. Fire performance of blind-bolted connections to concrete filled tubular columns in tension. Engineering structures 2015;96:111-125. http://dx.doi.org/10.1016/j.engstruct.2015.03.06

[11]   Tizani W, Al-Mughairi A, Owen JS, Pitrakkos T. Rotational stiffness of a blind-bolted connection to concrete-filled tubes using modified Hollo-bolt. Journal of Constructional Steel Research 2013. 80(0): 317-331.

[12]   National Institute of Standards and Techology (NIST). Final Report on the collapse of the World Trade Center towers. USA: National Institute of Standards and Technology. 2005.

[13]   National Institute of Standards and Techology (NIST). Final Report on the collapse of the World Trade Center building 7. USA: National Institute of Standards and Technology. 2008.

[14]   Al-Jabri KS, Burgess IW, Lennon T, Plank RJ. Moment-rotation-temperature curves for semi-rigid joints. Journal of Constructional Steel Research 2005. 61(3): 281-303.

[15]   Al-Jabri KS, Seibi A, Karrech A. Modelling of unstiffened flush end-plate bolted connections in fire. Journal of Constructional Steel Research 2006. 62(1–2): 151-159.

[16]   Yu H, Burgess I, Davison J, Plank R. Experimental and Numerical Investigations of the Behavior of Flush End Plate Connections at Elevated Temperatures. Journal of Structural Engineering 2011. 137(1): 80-87.

[17]   Huang SS, Davison B, Burgess IW. High-temperature tests on joints to steel and partially-encased H-section columns. Journal of Constructional Steel Research 2013. 80: 243-251.

[18]   Jiao-Ting L, Guo-Qiang L, Guo-Biao L, Ling-zhu C. Experimental investigation on flush end-plate bolted composite connection in fire. Journal of Constructional Steel Research 2012. 76: 121-132.

Pascual A M, Romero M L, Tizani W. Fire performance of blind-bolted connections to concrete filled tubular columns in tension. Engineering structures 2015;96:111-125. http://dx.doi.org/10.1016/j.engstruct.2015.03.06

[19]   Wang YC, Dai XH, Bailey CG. An experimental study of relative structural fire behaviour and robustness of different types of steel joint in restrained steel frames. Journal of Constructional Steel Research 2011. 67(7): 1149-1163.

[20]   Dai XH, Wang YC, Bailey CG. Numerical modelling of structural fire behaviour of restrained steel beam-column assemblies using typical joint types. Engineering Structures 2010. 32(8): 2337-2351.

[21]   Ding J, Wang YC. Experimental study of structural fire behaviour of steel beam to concrete filled tubular column assemblies with different types of joints. Engineering Structures 2007. 29(12): 3485-3502.

[22]   Elsawaf S, Wang YC, Mandal P. Numerical modelling of restrained structural subassemblies of steel beam and CFT columns connected using reverse channels in fire. Engineering Structures 2011. 33(4): 1217-1231.

[23]   Pascual AM, Romero ML, Tizani W. Thermal behaviour of blind-bolted connectios to hollow and concrete filled tubular columns. Journal of Constructional Steel Research 2015. 107: 137-149.

[24]   Pawtucket RIH, Karlsson & Sorenson, Inc. ABAQUS. ABAQUS/Standard Version 6.6 User's Manual: Volumes I-III. 2005.

[25]   Bursi OS, Jaspart JP. Basic issues in the finite element simulation of extended end plate connections. Computers & Structures 1998. 69(3): 361-382.

[26]   Janss J, Jaspart JP, Maquoi R. Experimental study of the non-linear behaviour of beam-to-column bolted joints. Proc. of a State-of-the art workshop on connections and the behaviour, strength and design of steel structures. Elsevier Applied Science Publishers 1987: 26-32.

Pascual A M, Romero M L, Tizani W. Fire performance of blind-bolted connections to concrete filled tubular columns in tension. Engineering structures 2015;96:111-125. http://dx.doi.org/10.1016/j.engstruct.2015.03.06

[27]   Wang ZY, Tizani W, Wang QY. Strength and initial stiffness of a blind-bolt connection based on the T-stub model. Engineering Structures 2010. 32(9): 2505-2517.

[28]   Mesquita A, Da Silva LS, Jordao S. Behaviour of I beam-SHS column steel joints with hollo-bolts: An experimental study. Proc. 13th International Conference on Tubular Structures. Hong Kong, China. 2010.

[29]   Espinos A, Gardner L, Romero ML, Hospitaler A. Fire behaviour of concrete filled elliptical steel columns. Thin-Walled Structures 2011. 49(2): 239-255.

[30]   Shi G, Shi Y, Wang Y, Bradford MA. Numerical simulation of steel pretensioned bolted end-plate connections of different types and details. Engineering Structures 2008. 30(0): 2677-2686.

[31]   Cabrero JM. Nuevas Propuestas para el Diseño de Pórticos y Uniones Semirrígidas de Acero. Tesis doctoral (PhD), Universidad de Navarra, Spain. 2006.

[32]   Liu Y, Málaga-Chuquitaype C, Elghazouli AY. Response and component characterisation of semi-rigid connections to tubular columns under axial loads. Engineering Structures 2012. 41(0): 510-532.

[33]   Pawtucket RIH, Karlsson & Sorenson, Inc. ABAQUS. ABAQUS/Standard Version 6.6 User's Manual: Volumes V. 2005.

[34]   CEN. *EN 1992-1-1, Eurocode 2: Design of concrete structures. Part 1-1: General rules and rules for buildings.* Brussels, Belgium: Comité Européen de Normalisation. 2004.

[35]   FIB 2010. Model Code 2010. Lausanne, Switzerland: Fédération Internationale du Béton.

Pascual A M, Romero M L, Tizani W. Fire performance of blind-bolted connections to concrete filled tubular columns in tension. Engineering structures 2015;96:111-125. http://dx.doi.org/10.1016/j.engstruct.2015.03.06

[36]   ISO 834: Fire resistance tests, elements of building construction. Switzerland: International Standards Organisation. 1980.

[37]   Espinos A, Romero ML, Hospitaler A. Advanced model for predicting the fire response of concrete filled tubular columns. Journal of Constructional Steel Research 2010. 66(8-9): 1030-1046.

[38]   CEN. *EN 1994-1-2, Eurocode 4: Design of composite steel and concrete structures. Part 1-2: General rules - Structural fire design*. Brussels, Belgium: Comité Européen de Normalisation. 2005.

[39]   Kodur V, Kand S, Khaliq W. Effect of Temperature on Thermal and Mechanical Properties of Steel Bolts. Journal of Materials in Civil Engineering 2012. 24(6): 765-774.

[40]   CEN. *EN 1993-1-2, Eurocode 3: Design of steel structures. Part 1-2: General rules – Structural fire design*. Brussels, Belgium: Comité Européen de Normalisation. 2005.

[41]   Kirby BR. The behaviour of High-Strength Grade 8.8 Bolts in Fire. Journal of Constructional Steel Research 1995. 33(1-2): 3-38.

[42]   CEN. *EN 1992-1-2, Eurocode 2: Design of concrete structures. Part 1-2: General rules – Structural fire design*. Brussels, Belgium: Comité Européen de Normalisation. 2004.

[43]   Gonzalez F, Lange J. Behaviour of high strength grade 10.9 bolts under fire conditions. Proc. Int. Conference on Applications of Structural Fire Design. Prague, Czech Republic 2009.

[44]   Hanus F, Zilli G, Franssen JM. Behaviour of Grade 8.8 bolts under natural fire conditions-Tests and model. Journal of Constructional Steel Research 2011. 67(8): 1292-1298.

Pascual A M, Romero M L, Tizani W. Fire performance of blind-bolted connections to concrete filled tubular columns in tension. Engineering structures 2015;96:111-125. http://dx.doi.org/10.1016/j.engstruct.2015.03.06

[45]   Li GQ, Jiang SC, Yin YZ, Chen K, Li MF. Experimental studies on the properties of constructional steel at elevated temperatures. Journal of Structural Engineering-Asce 2003. 129(12): 1717-1721.

[46]   Sakumoto Y, Keira K, Furumura F, Ave T. Tests of Fire-Resistant Bolts and Joints. Journal of Structural Engineering 1993. 119(11): 3131-3150.

Pascual A M, Romero M L, Tizani W. Fire performance of blind-bolted connections to concrete filled tubular columns in tension. Engineering structures 2015;96:111-125. http://dx.doi.org/10.1016/j.engstruct.2015.03.06

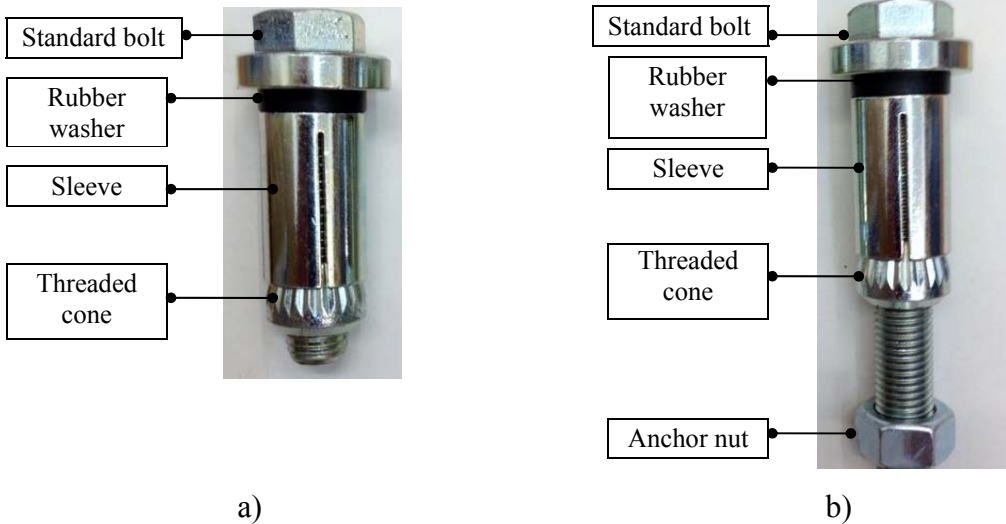a)   b)

Fig. 1. Blind-bolts: a) Hollo-bolt type, b) Extended Hollo-bolt type [23].

Pascual A M, Romero M L, Tizani W. Fire performance of blind-bolted connections to concrete filled tubular columns in tension. Engineering structures 2015;96:111-125. http://dx.doi.org/10.1016/j.engstruct.2015.03.06
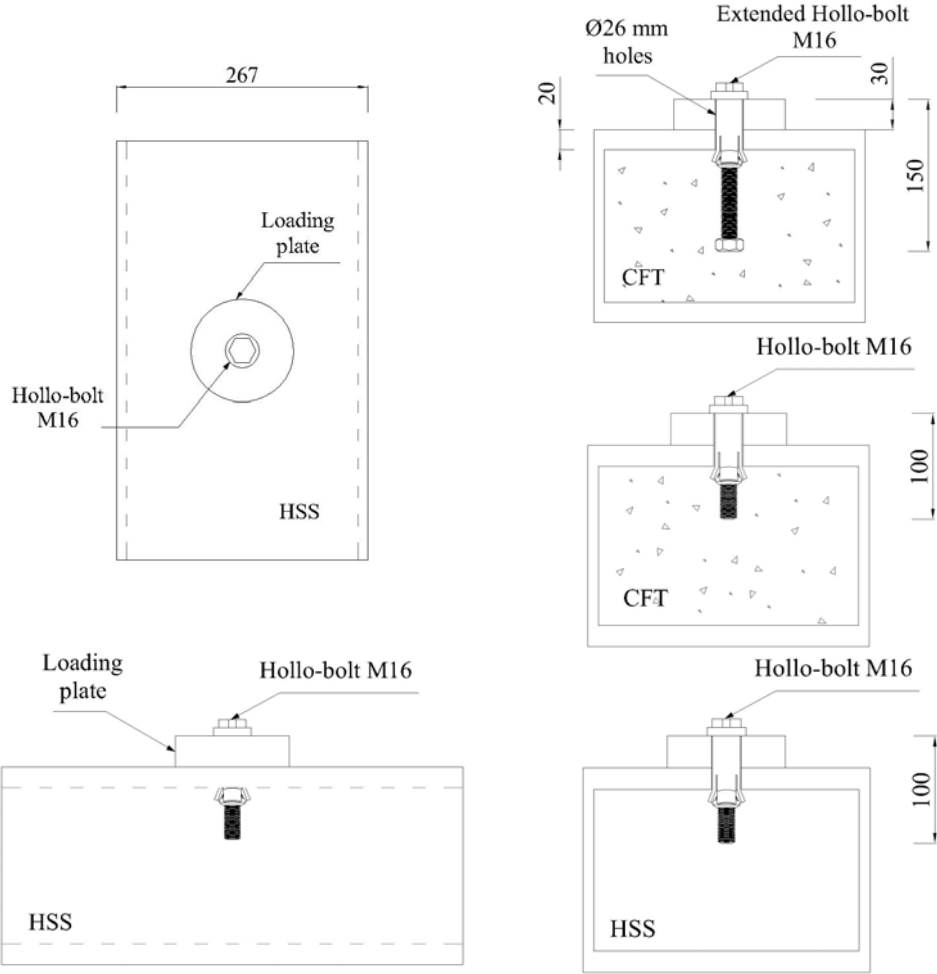
Fig. 2. Connection of a single blind-bolt (from tests [2])

Pascual A M, Romero M L, Tizani W. Fire performance of blind-bolted connections to concrete filled tubular columns in tension. Engineering structures 2015;96:111-125. http://dx.doi.org/10.1016/j.engstruct.2015.03.06
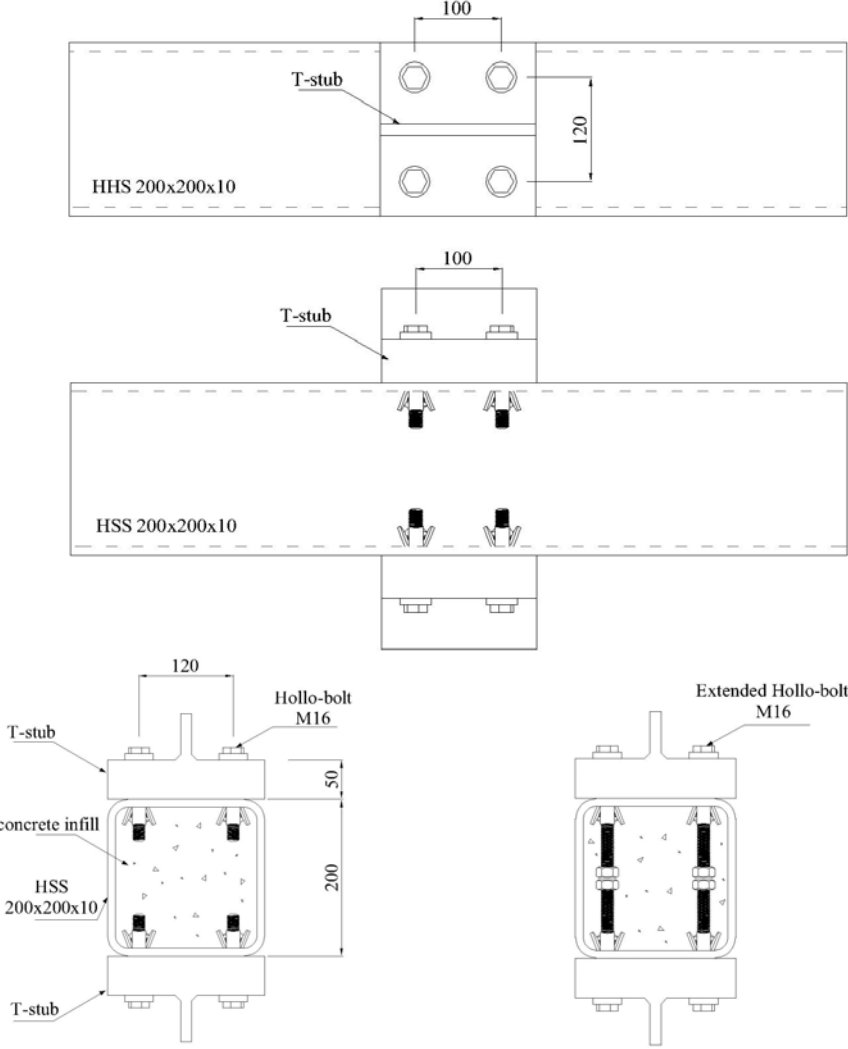
Fig. 3. Double T-stub connection to a HSS 200x200x10 (from tests [10]).
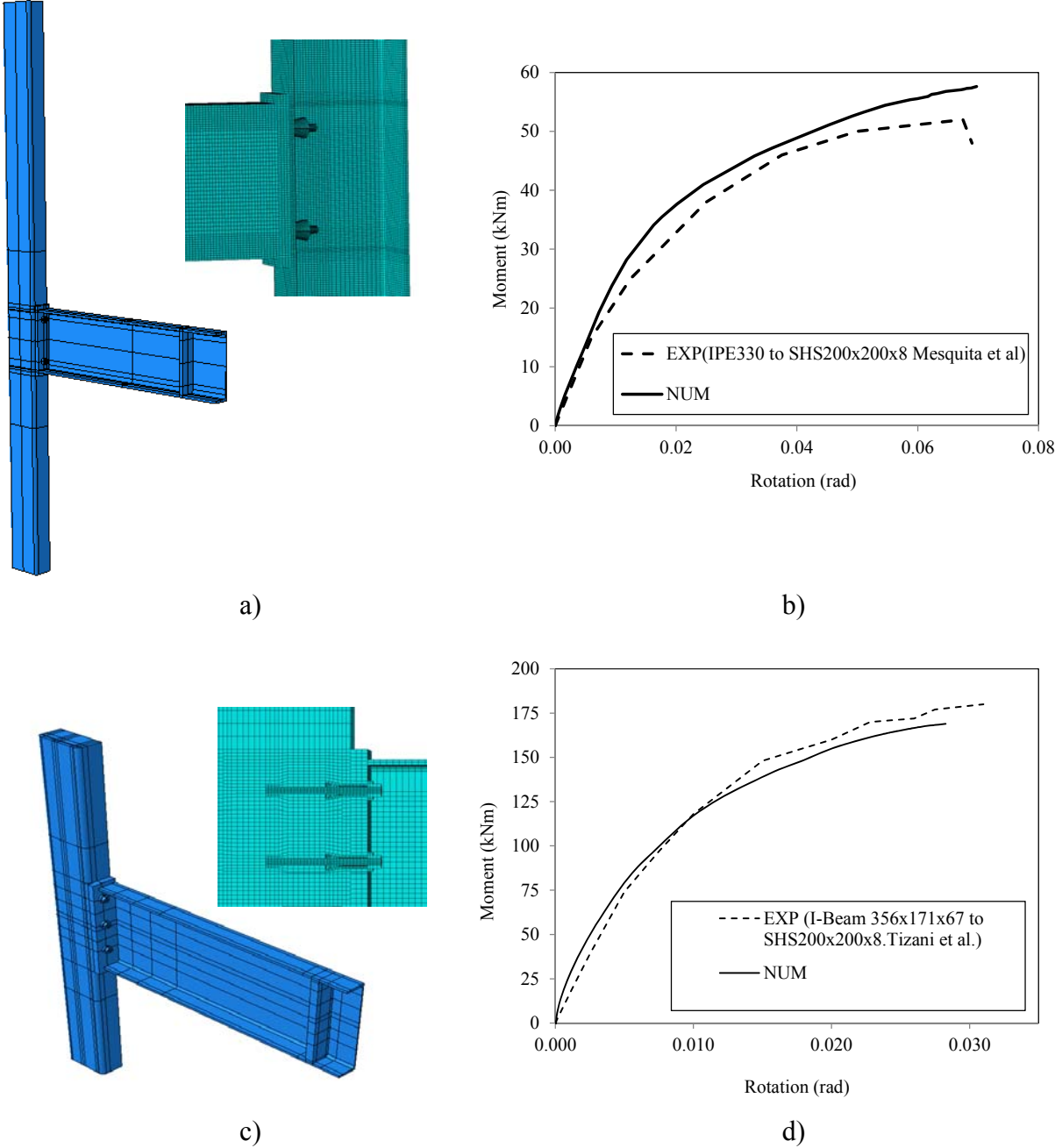
a)

b)

c)

d)

Fig. 4. a) FEM model of an I-beam to a HSS column connection; b) comparison with tests from Mesquita et al. [28]; c) FEM model of an I-beam to a CFT column connection; d) comparison with tests from Tizani et al. [11]

Pascual A M, Romero M L, Tizani W. Fire performance of blind-bolted connections to concrete filled tubular columns in tension. Engineering structures 2015;96:111-125. http://dx.doi.org/10.1016/j.engstruct.2015.03.06
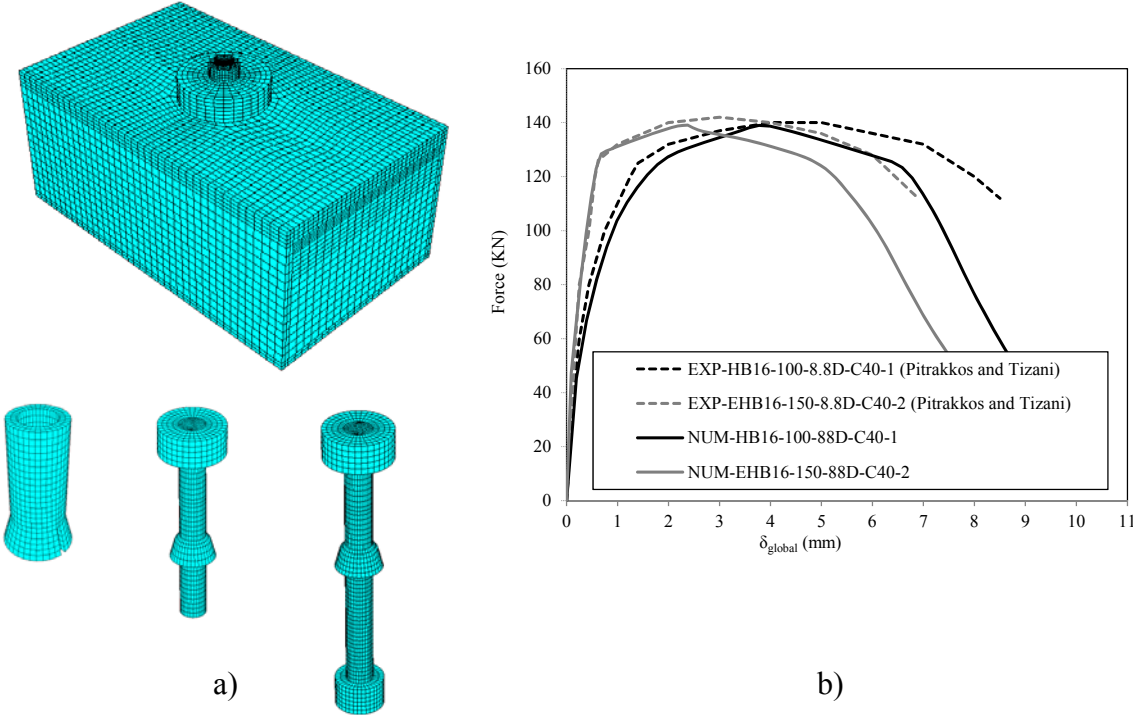
Fig. 5. a) Numerical model of the single blind-bolted connection at room temperature; b) comparison of force-displacement curve from FEM and test [2].
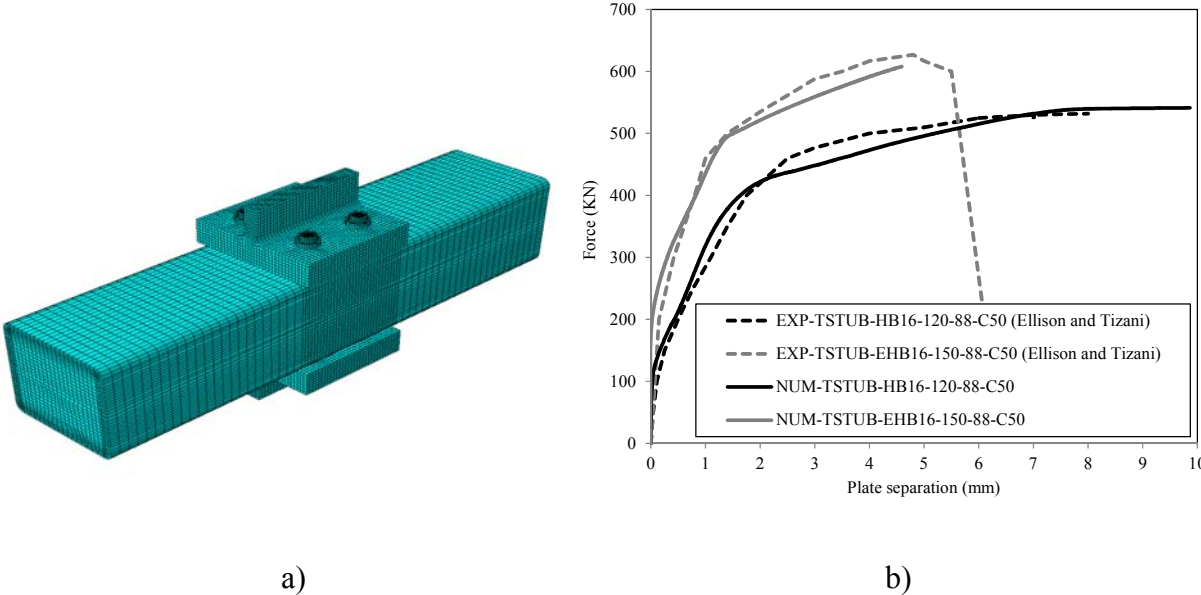

Fig. 6. a) Numerical model of the double T-stub connection to a CFT column at room temperature; b) comparison of force-displacement curve from FEM and test [10].

Pascual A M, Romero M L, Tizani W. Fire performance of blind-bolted connections to concrete filled tubular columns in tension. Engineering structures 2015;96:111-125. http://dx.doi.org/10.1016/j.engstruct.2015.03.06
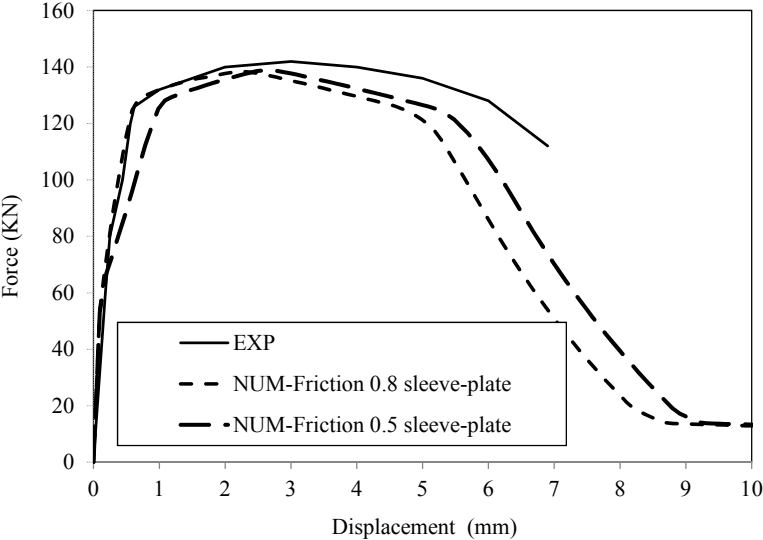
Fig. 7. Comparison of force-displacement curves of the EHB single blind-bolted connection using two different friction coefficients for the contact sleeve to plate hole surface.

Pascual A M, Romero M L, Tizani W. Fire performance of blind-bolted connections to concrete filled tubular columns in tension. Engineering structures 2015;96:111-125. http://dx.doi.org/10.1016/j.engstruct.2015.03.06

a)   b)

Fig. 8. a) Specimens inside the furnace after fire exposure; b) comparison of bolt temperature in EHB connection to CFT (Series 3) [23].

Pascual A M, Romero M L, Tizani W. Fire performance of blind-bolted connections to concrete filled tubular columns in tension. Engineering structures 2015;96:111-125. http://dx.doi.org/10.1016/j.engstruct.2015.03.06
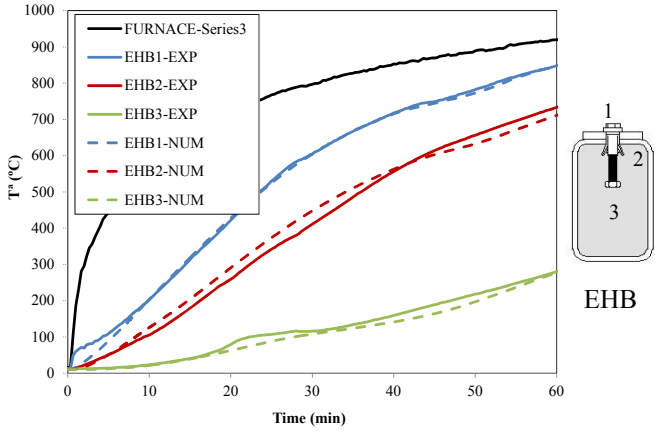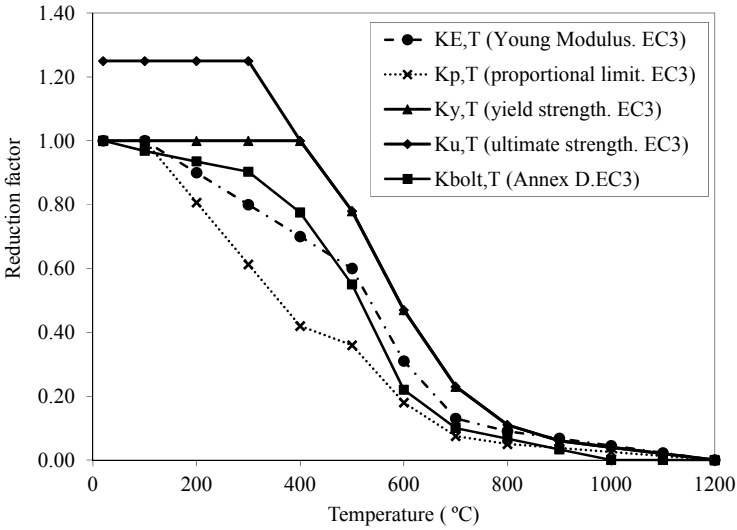
Fig. 9. Reduction factors from EC3 [40].

Fig. 10. Stress-strain relationship for steel bolts in the single blind-bolted connections at elevated temperatures.

Fig. 11. a) Mises stress (MISES,T), ultimate steel strength ($f_{u,T}$), and temperatures (T) along shank for the three cases of the single blind-bolted connections at connection failure; b) Mises stress (MISES,T), ultimate steel strength (fu,T), and temperatures (T) along sleeve for the three cases of the single blind-bolted connections at connection failure.

    a)HSS connection   b)HB to CFT column   c)EHB to CFT column
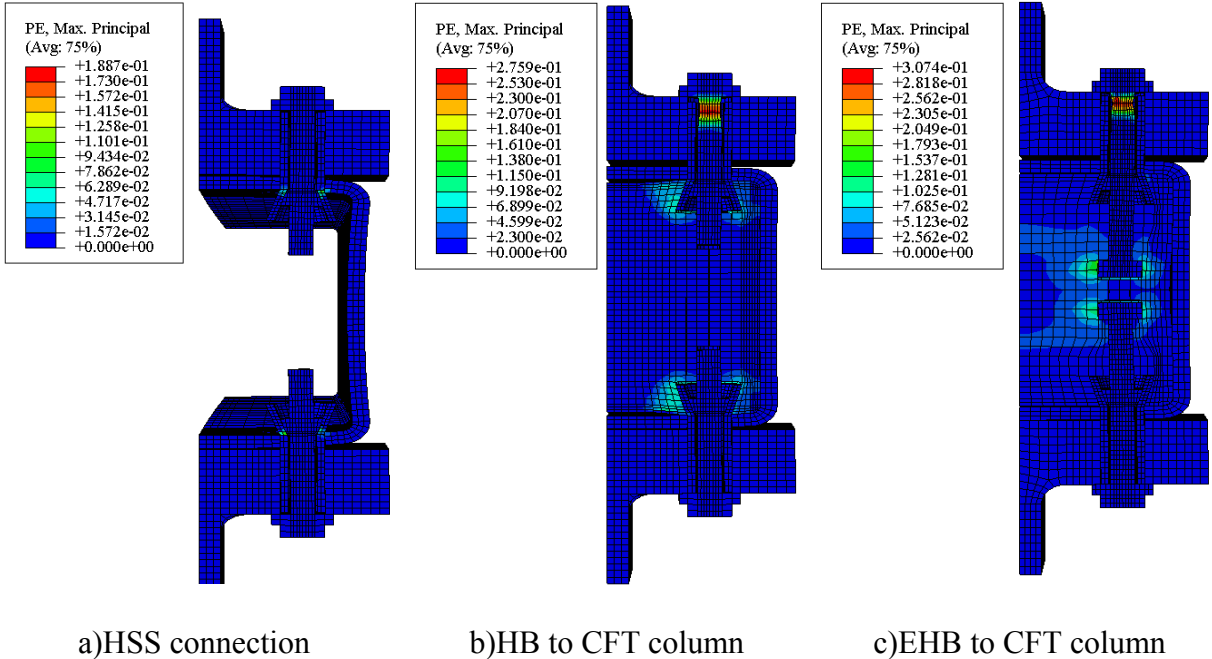
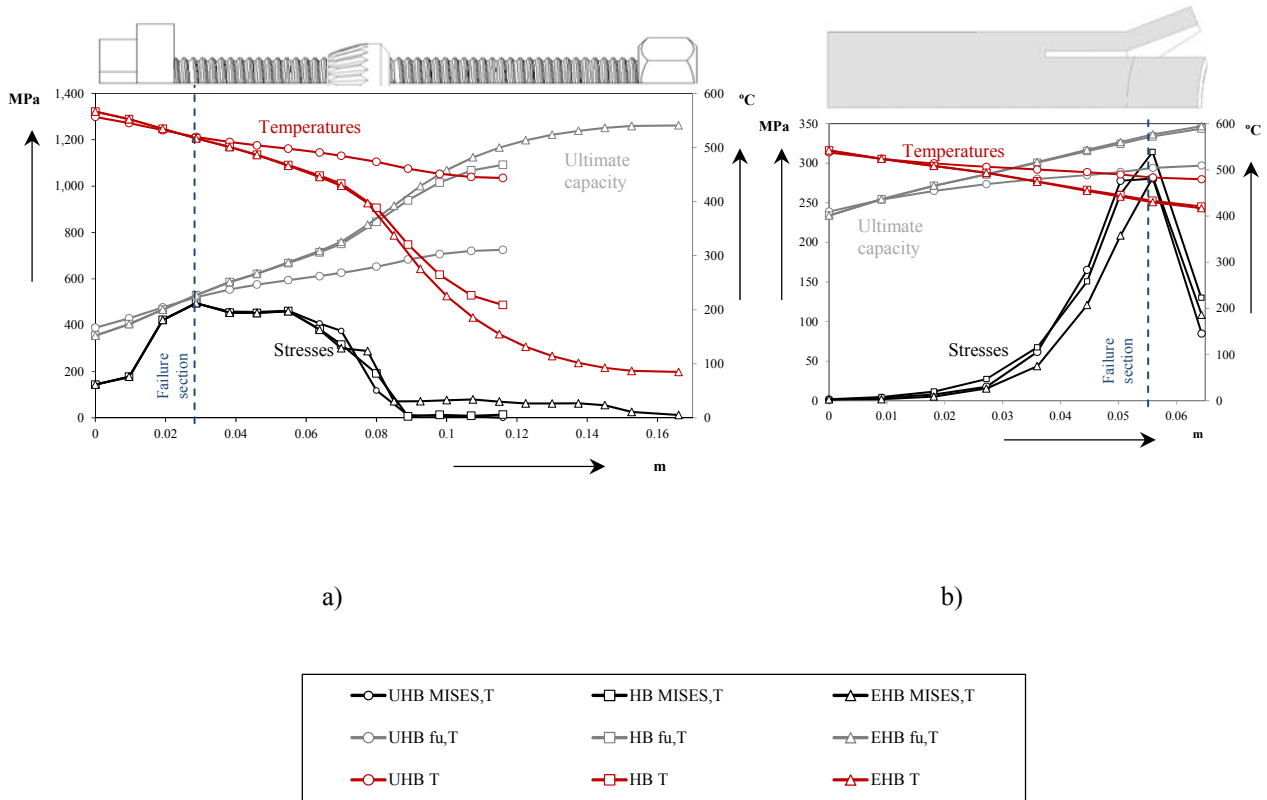Fig. 12. Plastic strain in double T-stub connections to tube column at failure.
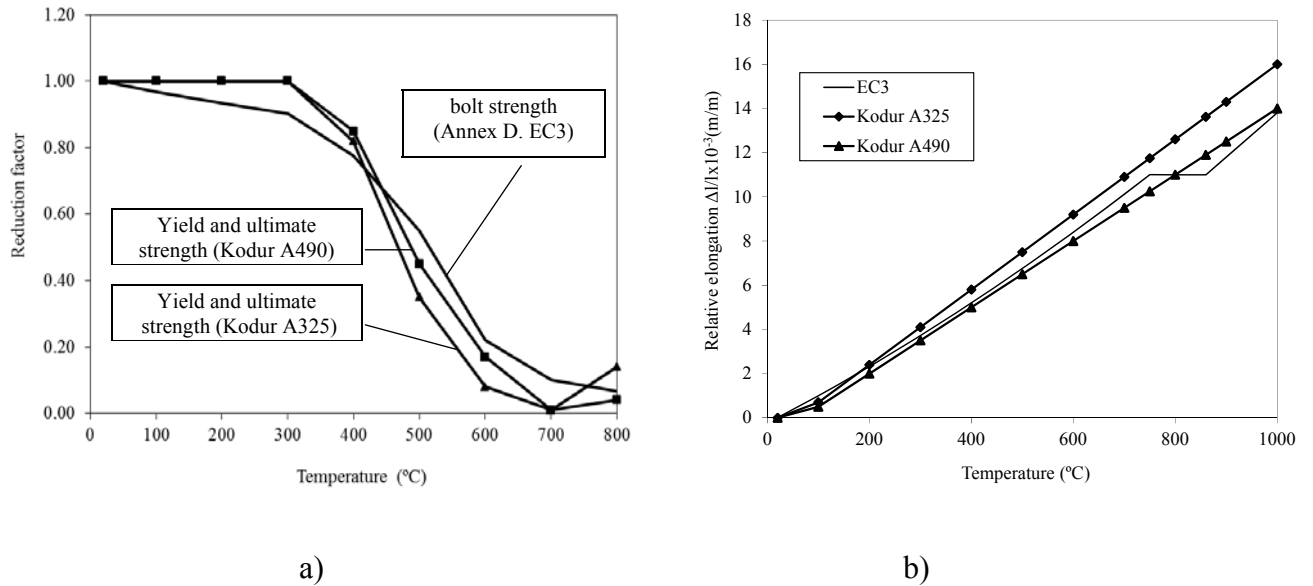
Pascual A M, Romero M L, Tizani W. Fire performance of blind-bolted connections to concrete filled tubular columns in tension. Engineering structures 2015;96:111-125. http://dx.doi.org/10.1016/j.engstruct.2015.03.06

a)   b)

Fig. 13. a) Comparison of strength reduction factors from Kodur [39] and EC3 [40]; b) comparison of thermal elongation from Kodur [39] and EC3 [40].
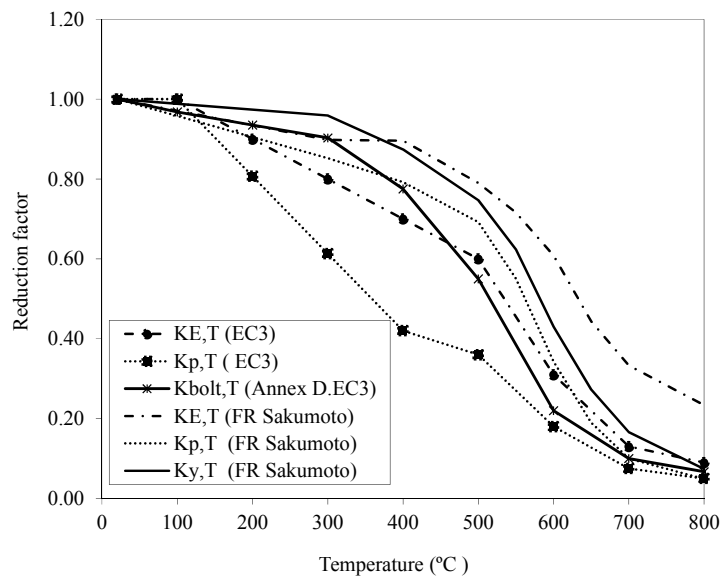
Fig. 14. Comparison between reduction factors from EC3 Annex D [40] and for fire resistance

Pascual A M, Romero M L, Tizani W. Fire performance of blind-bolted connections to concrete filled tubular columns in tension. Engineering structures 2015;96:111-125. http://dx.doi.org/10.1016/j.engstruct.2015.03.06

steel bolts from Sakumoto et al. [46].

Fig. 15. Comparison of force- bolt displacement curve at different temperatures for the single blind-bolted connections.

Fig. 16. Comparison of force-plate separation curve at different temperatures for the double T-stub to the tube column connections.

Pascual A M, Romero M L, Tizani W. Fire performance of blind-bolted connections to concrete filled tubular columns in tension. Engineering structures 2015;96:111-125. http://dx.doi.org/10.1016/j.engstruct.2015.03.06

Table 1.   List of the preliminary calibrated connection models at room temperature.

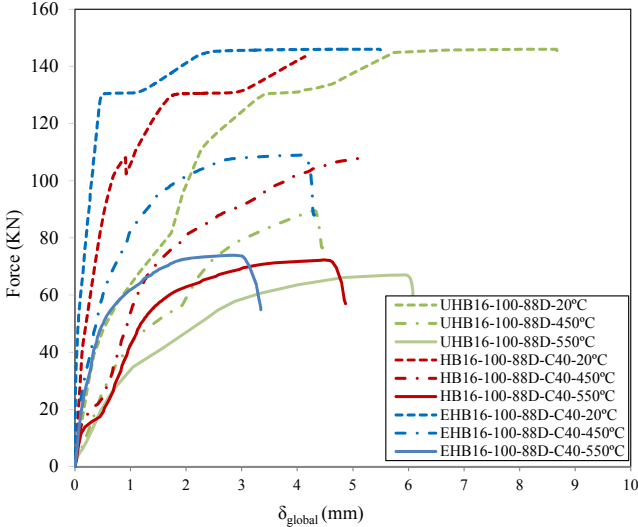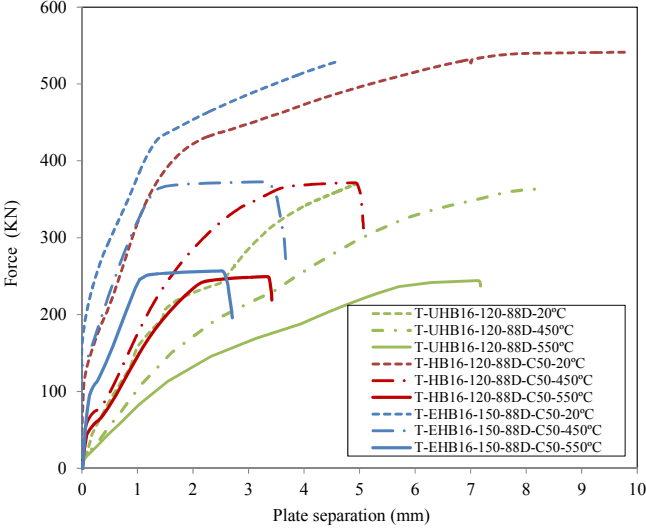| Type of connection	Calibration test (authors)	Type of bolt	Beam	Beam/Column	$\xi=M_{u,test}/M_{u,FEM}$ $(N_{u,test}/N_{u,FEM})$
2 T-stub	Bursi and Jaspart [25]	M12 grade 8.8	IPE 300	IPE 300	0.93
Flush endplate	Janss et al[26]	M16 grade 10.9	IPE 300	HEB160	1.01
2 T-stub	Wang et al[27]	M16 grade 8.8	I-section t=15 mm	I-section t=15 mm	0.98
2 T-stub	Wang et a[27]l	HB16 grade 8.8	I-section t=25 mm	I-section t=25 mm	1.02
Flush endplate	Mesquita et al[28]	HB20 grade 8.8	IPE 330	SHS 200x200x8	0.90
Flush endplate	Tizani et al[11]	EHB16 grade 8.8	356x171x67	CFT 200x200x12.5 (f_c=40N/mm^2)	1.05
Flush endplate	Tizani et al[11]	EHB16 grade 8.8	457x152x52	CFT 200x200x10 (f_c=40N/mm^2)	0.99
Extended endplate	Tizani et al[11]	EHB16 grade 8.8	356x171x67	CFT 200x200x10 (f_c=40N/mm^2)	1.05
Flush endplate	Tizani et al[11]	EHB16 grade 8.8	457x152x52	CFT 200x200x8 (f_c=40N/mm^2)	0.96
Flush endplate	Tizani et al[11]	EHB16 grade 8.8	356x171x67	CFT 200x200x8 (f_c=40N/mm^2)	1.05
Flush endplate	Tizani et al[11]	EHB16 grade 8.8	457x152x52	CFT 200x200x12.5 (f_c=40N/mm^2)	1.05
Flush endplate	Tizani et al[11]	EHB16 grade 8.8	356x171x67	CFT 200x200x10 (f_c=40N/mm^2)	1.08
Flush endplate	Tizani et al[11]	EHB16 grade 8.8	356x171x67	CFT 200x200x10 (f_c=60N/mm^2)	1.07

Pascual A M, Romero M L, Tizani W. Fire performance of blind-bolted connections to concrete filled tubular columns in tension. Engineering structures 2015;96:111-125. http://dx.doi.org/10.1016/j.engstruct.2015.03.06

Table 2.   List of single blind-bolted connections and the double T-stub connections calibrated at room temperature.

Specimen designation	Shank length	bolt grade	f_c	Maximum load (KN)		$\xi = N_{u,test}/N_{u,FEM}$
	(mm)		(MPa)	$N_{u,test}$	$N_{u, FEM}$	
Single blind-bolted connections						
Type HB (without concrete)						
HB16-100-8.8D-0-1	100	8.8		139	129	1.08
Type HB (concrete-filled)						
HB16-100-8.8D-C40-1	100	8.8	40	140	138	1.01
HB16-100-8.8D-C60-1	100	8.8	60	142	139	1.02
HB16-100-10.9E-C40-1	100	10.9	40	175	168	1.04
Type M (concrete-filled)						
M16-150-8.8D-C40-3	150	8.8	40	142	128	1.11
Type EHB (concrete-filled)						
EHB16-150-8.8D-C40-2	150	8.8	40	142	137	1.04
EHB16-150-8.8D-C60-1	150	8.8	60	140	138	1.01
EHB16-150-10.9E-C40-1	150	10.9	40	176	168	1.05
T-stub blind-bolted connections						
Type HB (concrete-filled)						
T-HB16-120-88D-C50	120	8.8	50	532	540	0.99
Type EHB (concrete-filled)						
T-EHB16-150-88D-C50	150	8.8	50	627	606	1.03

Table 3.   Mechanical properties of the steels in the single blind-bolted connections and the double T-stub connections and their source.

	f_y (MPa)	f_u (MPa)	E (GPa)	v	Reference
Single blind-bolted connections					
Plates	440	517	205	0.3	Tizani et al. [11]
Sleeve bolt	382	512	210	0.3	Liu et al. [32]
Shank bolt	836	931	207	0.3	Pitrakkos and Tizani [2]
T-stub blind-bolted connections					
SHS	440	517	205	0.3	Tizani et al. [11]
Sleeve bolt	382	512	210	0.3	Liu et al. [32]
Shank bolt HB	692	865	210	0.3	Ellison and Tizani [10]
Shank bolt EHB	793	992	210	0.3	Ellison and Tizani [10]

Pascual A M, Romero M L, Tizani W. Fire performance of blind-bolted connections to concrete filled tubular columns in tension. Engineering structures 2015;96:111-125. http://dx.doi.org/10.1016/j.engstruct.2015.03.06

Table 4.   List of connections simulated under fire conditions.

Specimen index	Type of connection	Type of bolt	Type of column	Variables
UHB16-100-8.8D	single bolt	HB	HSS	load level, steel bolt (EC3/Kodur/FR)
HB16-100-8.8D-C40	single bolt	HB	CFT	load level, steel bolt (EC3/Kodur/FR)
EHB16-100-8.8D-C40	single bolt	EHB	CFT	load level, steel bolt (EC3/Kodur/FR)
T-UHB16-100-8.8D	double T-stub	HB	HSS	steel bolt (EC3/FR)
T-HB16-100-8.8D-C50	double T-stub	HB	CFT	steel bolt (EC3/FR)
T-EHB16-100-8.8D-C50	double T-stub	EHB	CFT	steel bolt (EC3/FR)

Table 5.   FRR for single blind-bolted connections and T-stub connections. Load level influence for single blind-bolted connections.

Specimen index	Load level	FRR	$FRR_{HB/EHB}$-FRR_{UHB}	
	%	min	min	%
UHB16-100-8.8D-L50	50	20.55		
UHB16-100-8.8D-L40	40	23.15		
UHB16-100-8.8D-L20	20	30.78		
HB16-100-8.8D-C40-L50	50	24.68	4.13	20.12%
HB16-100-8.8D-C40-L40	40	27.01	3.87	16.71%
HB16-100-8.8D-C40-L20	20	35.60	4.82	15.67%
EHB16-150-8.8D-C40-L50	50	24.70	4.15	20.21%
EHB16-150-8.8D-C40-L40	40	27.14	4.00	17.27%
EHB16-150-8.8D-C40-L20	20	35.63	4.85	15.77%
T-UHB16-120-8.8D	50	17.78		
T-HB16-120-8.8D-C50	50	22.15	4.37	24.55%
T-EHB16-120-8.8D-C50	50	22.05	4.27	23.99%

Pascual A M, Romero M L, Tizani W. Fire performance of blind-bolted connections to concrete filled tubular columns in tension. Engineering structures 2015;96:111-125. http://dx.doi.org/10.1016/j.engstruct.2015.03.06

Table 6.   Effect on FRR of using Kodur properties and FR steel bolts in single blind-bolted and in T-stub connections.

Specimen index	FRR	FRR_{Kodur}-FRR_{EC3}		FRR_{FR}-FRR_{EC3}		FRR_{CFT}-FRR_{HSS}	
	min	min	%	min	%	min	%
UHB16-100-8.8D-EC3	20.55						
UHB16-100-8.8D-Kodur	18.33	2.22	10.79%				
UHB16-100-8.8D-FR	21.48			0.93	4.54%		
HB16-100-8.8D-C40-EC3	24.68					4.13	20.11%
HB16-100-8.8D-C40-Kodur	21.87	2.82	11.41%			3.53	19.27%
HB16-100-8.8D-C40-FR	28.83			4.15	16.81%	7.35	34.21%
EHB16-150-8.8D-C40-EC3	24.03					3.48	16.95%
EHB16-150-8.8D-C40-Kodur	21.88	2.15	8.95%			3.55	19.36%
EHB16-150-8.8D-C40-FR	28.88			4.85	20.18%	7.40	34.45%
T-UHB16-120-8.8D	17.78						
T-UHB16-120-8.8D-FR	17.78						
T-HB16-120-8.8D-C50	22.15					4.37	24.55%
T-HB16-120-8.8D-C50-FR	24.10			1.95	8.80%	6.32	35.52%
T-EHB16-120-8.8D-C50	22.05					4.27	23.99%
T-EHB16-120-8.8D-C50-FR	30.13			8.08	36.66%	12.35	69.45%

LIST OF FIGURE CAPTIONS

Fig. 1   Blind-bolts: a) Hollo-bolt type, b) Extended Hollo-bolt type [23].

Fig. 2   Connection of a single blind-bolt (from tests [2]

Fig. 3   Double T-stub connection to a HSS 200x200x10 (from tests [10]).

Fig. 4   a) FEM model of an I-beam to a HSS column connection; b) comparison with tests from Mesquita et al. [28]; c) FEM model of an I-beam to a CFT column connection; d) comparison with tests from Tizani et al. [11]

Fig. 5   a) Numerical model of the single blind-bolted connection at room temperature; b) comparison of force-displacement curve from FEM and test [2]

Fig. 6   a) Numerical model of the double T-stub connection to a CFT column at room temperature; b) comparison of force-displacement curve from FEM and test [10]

Fig. 7 Comparison of force-displacement curves of the EHB single blind-bolted connection using two different friction coefficients for the contact sleeve to plate hole surface

Fig. 8   a) Specimens inside the furnace after fire exposure; b) comparison of bolt temperature in EHB connection to CFT (Series 3) [23].

Fig. 9   Reduction factors from EC3

Fig. 10   Stress-strain relationship for steel bolts in the single blind-bolted connections at elevated temperatures.

Fig. 11   a) Mises stress (MISES,T), ultimate steel strength ($fu_{,T}$), and temperatures (T) along shank for the three cases of the single blind-bolted connections

Fig. 12   Plastic strain in double T-stub

Fig. 13   a) Comparison of strength reduction factors from Kodur [39] and EC3 [40]; b) comparison of thermal elongation from Kodur [39] and EC3 [40]

Fig. 14   Comparison between reduction factors from EC3 Annex D [40] and for fire resistance steel bolts from Sakumoto et al. [46].

Fig. 15   Comparison of force- bolt displacement curve at different temperatures for the single blind-bolted connections.

Fig. 16   Comparison of force-plate separation curve at different temperatures for the double T-stub to the tube column connection

LIST OF TABLE CAPTIONS

Table 1   List of the preliminary calibrated connection models at room temperature

Table 2   List of single blind-bolted connections and the double T-stub connections calibrated at room temperature.

Table 3   Mechanical properties of the steels in the single blind-bolted connections and the double T-stub connections and their source

Table 4   List of connections simulated under fire conditions

Table 5   FRR for single blind-bolted connections and T-stub connections. Load level influence for single blind-bolted connections

Table 6   Effect on FRR of using Kodur properties and FR steel bolts in single blind-bolted and in T-stub connections.